RESEARCH ARTICLE OPEN ACCESS

Multifractal-Based Featuresfor Medical ImagesClassification

Saad Al-Momen[1] , Loay E. George[2], Raid K. Naji[3]
Computer Science Department, College of Science,
Baghdad University, IRAQ

--************************----------------------------------

Abstract:

This paper presents a method to classify colored textural images of skin tissues. Since medical images have highly heterogeneity, the development of reliable skin-cancer detection process is difficult, and a mono fractal dimension is not sufficient to classify images of this nature. A multifractal-based feature vectors are suggested here as an alternative and more effective tool. At the same time multiple color channels are used to get more descriptive features.

Two multifractal based set of features are suggested here. The first set measures the local roughness property, while the second set measure the local contrast property.A combination of all the extracted features from the three color models gives a highest classification accuracy with 99.4048% for training and 95.8333% for testing.

Keywords:-**Texture Classification, Texture Analysis, Fractal, Multifractal, Wavelet Features**

--************************----------------------------------

I. INTRODUCTION

A TUMOR IS RECOGNIZED AS THE EXISTENCE OF AN ABNORMAL MASS OF TISSUE WITH A CAPACITY FOR PROGRESSIVE GROWTH. IT IS A TERM USED TO DESCRIBE BODY CELL CHAOTIC GROWTH AND DIVISIONS OCCURRING IN AN UNCONTROLLABLE FASHION, USUALLY DUE TO CELL DNA CHANGE OR DAMAGE [1]. TUMORS CAN BE CLASSIFIED INTO TWO MAIN CLASSES OF BENIGN OR MALIGNANT [2]:

- Benign (not cancer): Benign tumors are rarely life-threatening, and theydo not spread to other parts of the body. They often can be removed andusually do not grow back.
- Malignant (cancer): Malignant tumors can harm nearby tissues andspread to other parts of the body.

According to the World Health Organization (WHO), malignant tumor or cancer is the leading causes of morbidity and mortality worldwide, with approximately 14 million new cases and 8.2 million cancer related deaths in 2012. The number of new cases is expected to rise by about 70% over the next 2 decades [3]. There are as many different types of tumors as there are different types of human cells, just over 200 types, with some being very common, while others are extremely rare [2]. Nearly all tumors are named after the organ or type of cell that they originate from.

Cancer arises from one single cell that takes a multistage process to transform from a normal cell into a tumor cell, typically a progression from a pre-cancerous lesion to malignant tumors. These changes are the result of the interaction between a person's genetic factors with the physical, chemical, and biological carcinogens.

Cancer mortality can be reduced if cases are detected and treated early. The appearance of body organs in addition to other medical tests, such as biopsy specimens, body fluid analysis and measurement of body functions, can be significant for physicians to reach to a decision on the medical situation of the patient. Physicians can have an initial idea on the normality orabnormality of the observed organ from its general appearance via an image captured. Image texture is one of the important cues that could give physicians such indication, which would trigger certain treatment procedures, if texture is found abnormal, depending on the nature of the disease.

To avoid diagnosing disease at an advanced stage when it has already progressed and hence patient's prognosis becomes poor, early detection of disease can be improved by using effective clinical diagnosis systems.

II. SKIN CANCER

Skin cancers are named for the type of cells where the cancer starts. It is also known as skin neoplasia. Skin cancer is a change in some of the cells of skin such that they grow abnormally to form a malignant tumor. These abnormal cells can invade through the skin into adjacent structures or travel throughout body and become implanted in other organs and continue to grow; a process called metastasis [4].

There are three common types of skin cancer, basal cell carcinoma (BCC), squamous cell carcinoma (SCC) and melanoma. There are other types, but they considered more rare forms of skin cancer. BCC and SCC are the most common forms of skin cancer; and they are together referred to as non-melanoma skin cancer. While, Melanoma is generally the most serious form of skin cancer because it tends to spread (metastasize) throughout the body quickly [5].

Figure 2 shows sample examples of the skin tissue classes that used in this study.These images were taken from stained sections (glass slides) of skin cancer biopsy cases from different Iraqi hospital pathology departments. Taking images from these sections was conducted through using microscope-attached digital camera; it was performed with the help of an experienced pathologist. The pathologist was required to pin-point the areas of interest in histological [4].It is clear that the tissue structure is not identical in all image samples and varies from one patient to another, since disease might alter the tissue structure unequally. This tissue heterogeneity places tissue patterns commonly in the category of stochastic or possibly fractal textures.

Generally speaking, the image textures of human-organ tissues are complicated as anything in nature, and digital microscopic images of these tissues show highly irregular texture patterns with the variation of the image resolution. It is possible that different types of texture may have the same fractal dimension; so, it is difficult to realize the pathological changes located in different organs only by methods based on single fractal, especially or the textures that possess similar fractal dimension.

Also, the fractal dimension of such type of texture images is not constant over all scales, but rather over small ranges of scales. Furthermore, the cell's texture patterns vary with the type of the cancer or the grade of the cancer which makes image analysis for tissue and cell images is complicated and challenging. Therefore, one has to generalize the analysis with applying more advanced mathematical techniques.

This paper analysis the skin tissue medical images from the multifractal point of view. Many researchers conclude that multifractal technique is an effective and robust tool for image classification [6], [7], [8], [9], [10] and [11]. Therefore, multifractal technique has been widely applied in biomedical image processing. Multifractal describes the fractal properties of an image using an intensity-based measure within the neighborhood of each pixel. Although there is a link between roughness and fractal dimension, the roughness is not sufficient to describe a textured surface, because other characteristics have to be involved, such as arrangements and spatial distribution of grey levels. Multifractal theory can avoid the drawback of the single fractal dimension.

In multifractal, instead of one measure, ?, describing the phenomenon in all scales using fractal approach, the set of measures, ??i, arise, describing statistically the same phenomenon in different scales.

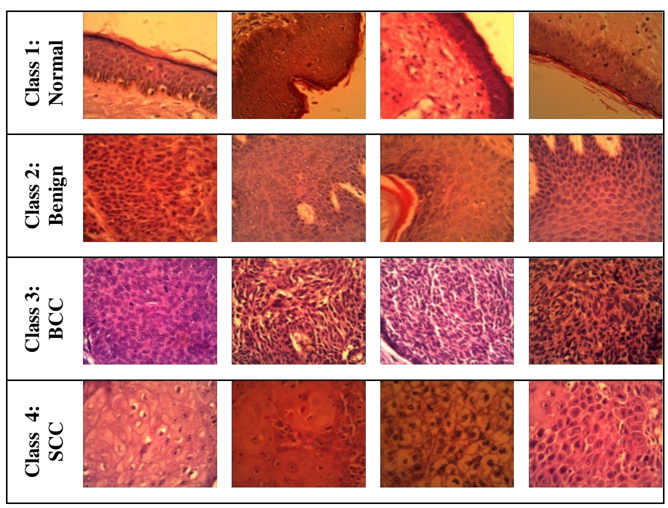

Figure1. Sample examples of the skin tissue classes

III. PROPOSED SCHEME

To classify the skin cancer tissues, two multifractal based set of features are suggested. The first set measures the local roughness property, while the second set measure the local contrast property. These set of features are extracted from multiple color channels in order to get more informative feature vectors and to cover the heterogeneity of the studied textures.Three color channels (X_1, X_2, X_3) were taken for each image in addition to their corresponding brightness (gray). Three color systems were studied here: *RGB*, *Lab*, and *HSV* [12] and [13]. According to that, the four channels will be taken in this study are (*R*, *G*, *B*, *g*) , (*L*, *a*, *b*, *g*), and (*H*, *S*, *V*, *g*) corresponding to the *RGB*, *Lab*, and *HSV* system, respectively.

Figure (2) shows that the input image is passed through the following main steps:

1- Decomposing the original image into 3 color channels and 1 gray channel depending on the chosen color system.
2- For each one of the four channels, two feature vectors are calculated:
   a. The local roughness feature vector F_1.
   b. The local contrast feature vector F_2.
3- The two feature vectors F_1 and F_2 are used individually or to gather to establish the classification task.

During the training phase, three templates are constructed for each class to cope over the variability of the images in each class. The conducted experiments showed that using one or two templates may not always enough for efficient classification. In this research paper, three initial templates have been chosen as: (i) IC_1, which is the mean feature vector of all the feature vectors extracted from the training samples belong to the class, (ii) IC_2, the farthest feature vector to IC_1, and (iii) IC_3, the farthest feature vector to both IC_1&IC_2. Then the K-means algorithm is used to improve the values of these initial templates [14], and [15].

Commonly, Euclidean distance measure is used to match the similarity. But, one weakness of the basic Euclidean distance function is that if one of the input features has a relatively large range, then it can overpower the other features. Since the problem here is the used features are not isotropic; that is, every feature may not have similar behaviors. So, the normalized Euclidean distance has been used to evaluate the similarity degree between the extracted feature vector of the tested sample, and the templates representing certain class [14] and [15]:

$$d\left(T^i, F^j\right) = \sqrt{\sum_{k=1}^{K} \frac{\left(T_k^i - F_k^j\right)^2}{\sigma_k}} \quad (1)$$

Where, T_k^i is the template value of k^{th} feature that belong to i^{th} class; F_k^j is the value of k^{th} feature extracted from j^{th} sample; σ_k is the standard devotion over the sample set.

As mentioned above, the matching process uses three templates per class, in order to maximize the probability of true match classification and minimize the misclassification. The efficiency of classification is calculated for each distance using the following equation [16]:

$$\eta(\%) = \frac{\text{Total no.of samples} - \text{No.of misclassified samples}}{\text{Total no.of samples}} \times 100\%$$

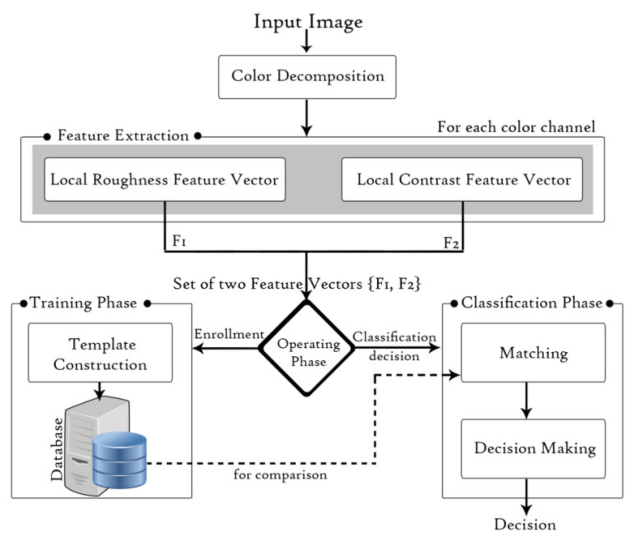

IV. FEATURES EXTRACTION

Two multifractal based set of features are suggested here. The first set measures the local roughness property, while the second set measure the local contrast property.

A. Local Roughness Features

Roughness is a component of surface texture. It is measured by the deviations in the direction of the normal vector of a real surface from its ideal form. The surface is considers as rough surface when the deviations are large; otherwise it is smooth.

The human-organ tissues have high heterogeneity nature, so the roughness is different from part to part. Local roughness features are suggested here to cover this issue. This set of features depends on the local variations in the pixels' values relative to their local position in the image. The original image of size $m\times n$ is divided into blocks of size $b\times b$, where b is an odd number. The differences between the pixel's value in the block's center and the pixels surrounding it considered as local roughness measure. After the local pixels differences are computed for each central pixel, two matrices*LRmin*() and *LRmax*() of size $\left\lfloor\frac{m}{b}\right\rfloor\times\left\lfloor\frac{n}{b}\right\rfloor$, are constructed to hold the minimum and maximum of these differences respectively.Then the fractal dimension for each of *LRmin*() and *LRmax*() are computed using the BCABH method[17]to produce two values *FD*(*LRmin*) and *FD*(*LRmax*); Figure (3)illustrates these steps.

The above procedure is repeated to all the color's channelX_1, X_2, X_3 and g to get a feature vector (F_1) that consists of eight values.

$$F_1=\{FD_{X_1}(LRmin),FD_{X_1}(LRmax),FD_{X_2}(LRmin),FD_{X_2}(LRmax),\\ FD_{X_3}(LRmin),FD_{X_3}(LRmax),FD_g(LRmin),\ FD_g(LRmax)\}$$

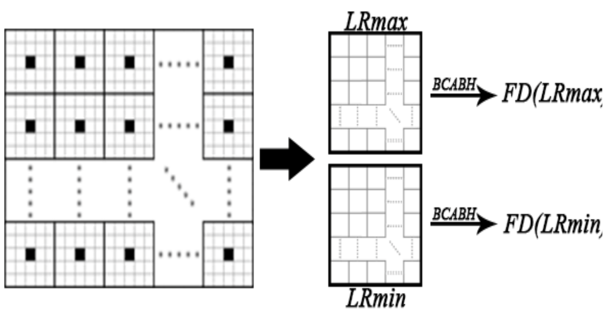

Figure 3. Fractal Dimension of Local Roughness

V. LOCAL CONTRAST FEATURES

Contrast is the difference in luminance or color that makes an objectdistinguishable. In visual perception of the real world, contrast is determined by the difference in the color and brightness of the object and other objects within the same field of view.

There are many possible definitions of contrast. Some include color; others do not. Michelson contrast [18] is considered here because it is usually used for patterns where both bright and dark features are equivalent and take up similar fractions of the area, which is the case of the studied tissues. The Michelson contrast is defined as

$$\frac{I_{max}-I_{min}}{I_{max}+I_{min}} \qquad (4)$$

with I_{max} and I_{min} representing the highest and lowest luminance.

A multifractal technique is used here, where a window of size w is centered at a pixel p and the contrast measure with respect to w can be characterized as follows:

$$\mu_p(w)=Dw^{\alpha_p} \qquad (5)$$

$$w=2i+1,\qquad i=0,1,2,\dots,d \qquad (6)$$

where$d$ is the total number of windows used to compute α_p.

$$\log(\mu_p)=\alpha_p\log(w)+\log(D) \qquad (7)$$

In other word,

$$y=\alpha_p x+C \qquad (8)$$

where $y=\log(\mu_p)$, $x=\log(w)$ and $C=\log(D)$.

It is clear from eq. (8) that α_p is the slope of the line, and it can be estimated using a linear regression

$$\alpha_p=\frac{n\cdot\sum xy-\sum x\cdot\sum y}{n\cdot\sum x^2-\sum x\cdot\sum x} \qquad (9)$$

Figure (4) illustrates the main steps to calculate the local contrast features, where:

1- The original image is divided into block of size $b\times b$, where b is an odd number.
2- For each block, α_p is calculated for the central pixel according to a predefined number of windows d. And the result is set in a matrix *Con*().
3- The fractal dimension of *Con*() is calculated using the BCABH method [17].

The above procedure is repeated to all the color's channelX_1, X_2, X_3 and g to get a feature vector (F_2) that consists of four values.

$$F_2=\{FD_{X_1}(Con),\ FD_{X_2}(Con),\ FD_{X_3}(Con),FD_g(Con)\} \qquad (10)$$

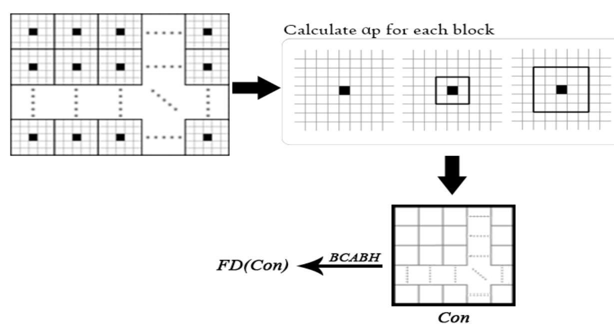

VI. EXPERIMENTAL RESULTS

In order to demonstrate the efficiency of the proposed classification system for the medical images, a number of experiments have been performed. 24 skin tissues are predefined by a pathologist into 4 main classes: 6 are Normal, 6 are Benign, 6 are Basal Cell Carcinoma (BCC) and 6 are Squamous Cell Carcinoma (SCC). Each tissue defines a separate subclass from the corresponding main class, and it is represented by 30 randomly selected colored images of size 128 x 128 pixels.7 randomly chosen samples from each class were used for training, while the rest 23 samples were used for testing the classifier. The conducted tests have been directed toward finding to which class the query image belongs.

The classification was in two stages. The first stage does the classification on the basis of 24 sub-classes. And in the second stage each sub-class is assigned to its corresponding main class.

Tables(1), (2) and (3) show the percentage of correctly classified samples of all the tested samples under the use of the local roughness feature vector (F_1), depending on the RGB, Lab and HSV color model, respectively.

- With the RGB model the highest percentage of correctly classified sample achieved with block of size b=17, and the values are 100% for training and 95.6522% for testing.
- With the Lab model the highest percentage of correctly classified sample achieved with block of size b=9, and the values are 97.619% for training and 92.3913% for testing.
- With the HSV model the highest percentage of correctly classified sample achieved with block of size b=9, and the values are 97.619% for training and 88.7681% for testing. At the same time there is a higher result with b=7, when excluding the gray channel, the accuracy values will be 98.2143% for training and 91.4855% for testing.

Tables (4), (5) and (6) show the percentage of correctly classified samples of all the tested samples under the use of the local contrast feature vector (F_2), depending on the RGB, Lab and HSV color model, respectively.

- With the RGB model the highest percentage of correctly classified sample achieved with number of windows d=1, and the values are 85.119% for training and 65.5797% for testing.
- With the Lab model the highest percentage of correctly classified sample achieved with number of windowsd=1, and the values are 88.0952% for training and 62.8623% for testing. At the same time there is a higher result with d=1, when excluding the gray channel, the accuracy values will be 99.4048% for training and 92.2101% for testing.
- With the HSV model the highest percentage of correctly classified sample achieved with number of windowsd=3, and the values are 95.8333% for training and 86.0507% for testing.

Tables (7), (8) and (9) show the percentage of correctly classified samples of all the tested samples under the use of the local roughness and local contrast feature vectors together $\{F_1, F_2\}$, depending on the RGB, Lab and HSV color model, respectively. The block size for the local roughness is fixed to b=9.

- With the RGB model the highest percentage of correctly classified sample achieved with number of windows d=1, and the values are 98.8095% for training and 88.587% for testing. At the same time there is a higher result with d=3, when excluding the gray channel, the accuracy values will be 99.8048% for training and 89.1304% for testing.
- With the Lab model the highest percentage of correctly classified sample achieved with number of windows d=3, and the values are 98.2143% for training and 90.942% for testing.At the same time there is a higher result with d=1, when excluding the gray channel, the accuracy values will be 100% for training and 92.2101% for testing.
- With the HSV model the highest percentage of correctly classified sample achieved with number of windows d=3, and the values are 95.8333% for training and 86.0507% for testing.

Tables (10), (11), (12), and (13) show the classification accuracy depending on the possible combination of the color models. A combination of all the extracted features from the three color models gives a highest classification accuracy with 99.4048% for training and 95.8333% for testing.

VII. CONCLUTIONS

According to the tests results presented in this paper, the following conclusions have been derived:

- The Local Roughness Feature Vector work better with the RGB color model. While The Local Contrast Feature Vector work better with the Lab color model.
- Excluding the gray channel from the RGB model enhance the performance of the Local Roughness Feature Vector classification. And excluding it

from the Lab model enhance the performance of the Local Contrast Feature Vector classification.

- A combination of the Local Roughness Feature Vector and the Local Contrast Feature Vector works better with the Lab model.
- Although the Local Contrast Feature Vector does not give a high accuracy classification but it supports the Local Roughness Feature Vector to raise the classification accuracy.
- A Combination of all the extracted features from the three color models gives highest classification accuracy as it is clear from Table (13).

VIII. REFERENCES

[1] Louis, C. J.; "Tumors: Basic principles and clinical aspects", Longman Group Limited, 1978.

[2] Sankar , D.; "Fractal Based Techniques for Classification of Mammograms and Identification of Microcalifications", PhD thesis, Cochin University of Science and Technology, India, 2011.

[3] Stewart, B. W.; and Wild, C. P.; "World Cancer Report 2014", World Health Organization (WHO), 2014.

[4] Abdul-Wadood, D. N.; George, L. E.; and Rashhed, N. A.; "Diagnosis of Skin Cancer Using Image Texture Analysis", International Journal of Scientific & Engineering Research, vol. 5, issue 6, June 2014.

[5] Siegel, R., Ma, J., Zou, a., and Jemal, A., "Cancer Statistics", A Cancer Journal for Clinicians, Vol. 64, No. 1, January/ February, 2014.

[6] Pentland, A.; "Fractal-based description of natural scenes", IEEE Transactions on Pattern Analysis and Machine Intelligence, 6 (6), pp. 661–674, 1984.

[7] Anh ,V. V.; Maedal , J.; Tieng, M.; and Tsui, T.; "Multifractal Texture Analysis and Classification", IEEE1999, Pp.445-449, 1999.

[8] Reljin, I. S., and Reljin, B. D.; "Fractal geometry and multifractals in analyzing and processing medical data and images", Archive of Oncology, 10(4), pp. 283-93, 2002.

[9] Nilsson, E.; "Multifractal-based Image Analysis with applications in Medical Imaging", Master’s Thesis in Computing Science and and Mathematics, Umeå University, Sweden, 2007.

[10] Lopes, R.; Betrouni, N.; "Fractal and Multifractal Analysis: A Review", Medical Image Analysis, Vol. 13, Pp. 634-649, 2009.

[11] Wang, Z., and Du, P.; "Multifractal Analysis and Modeling of Chaotic Channels", Journal of Software, vol. 7, no. 3, March 2012.

[12] Gonzalez, R. C.; Woods, R. E.; and Eddins, S. L.; "Digital Image Processing Using MATLAB", Second Edition, Gatesmark Publishing, 2009.

[13] Koschan, A., and Abidi, M.; "Digital color image processing", John Wiley, 2008.

[14] Al-Momen, S.; George, L.; Naji, R.; "The use of Gradient Based Features for Woven Fabric Images Classification", British Journal of Mathematics and Computer Science, Vol. 6, Issue 1, Pp. 68-78, 2015.

[15] Al-Momen, S.; George, L.; Naji, R.; "Texture classification using spline, wavelet decompositionand fractal dimension", Applied and Computational Mathematics, 4(1), Pp. 5-10, 2015.

[16] Bhiwani, R. J.; Khan, M. A.; Agrawal, S. M.; "Texture BasedPattern Classification", International Journal of Computer Applications, Vol. 1, No. 1, Pp. 54-56, 2010.

[17] Long, M.; and Peng, F.; "A Box-Counting Method with Adaptable Box Height for Measuring the Fractal Feature of Images"; Radio Engineering, Vol. 22, No. 1, Pp. 208-213, April 2013.

[18] Michelson, A.; "Studies in Optics", University of Chicago Press, 1927.

Table 1: The percentage of correctly classified samples under the local roughness feature vector (F_1) using the RGB color model

b	R-Channel		G-Channel		B-Channel		RGB-Channels		gray-Channel		All-Channels	
	Training	Testing	Training	Testing	Training	Testing	Training	Testing	Training	Testing	Training	Testing
3	75	53.2609	76.1905	55.7971	70.8333	52.3551	97.619	84.6014	78.5714	55.9783	97.619	86.413
5	67.8571	53.0797	72.0238	56.3406	73.2143	54.1667	96.4286	82.7899	73.2143	54.529	97.619	83.6957
7	72.619	55.6159	73.8095	55.4348	73.8095	51.087	95.2381	84.4203	73.8095	54.529	97.0238	84.6014
9	75	53.2609	76.1905	55.7971	70.8333	52.3551	97.619	84.6014	78.5714	55.9783	97.619	86.413
11	67.8571	50.1812	75	54.7101	70.2381	53.0797	97.0238	84.6014	76.7857	51.6304	97.619	83.3333
13	63.6905	49.8188	72.619	54.8913	64.2857	53.442	97.619	84.2391	73.8095	51.2681	98.2143	85.1449
15	66.6667	50.7246	78.5714	58.8768	78.5714	61.0507	98.8095	93.4783	64.2857	49.2754	99.4048	95.2899
17	64.881	44.7464	76.7857	57.2464	81.5476	60.3261	98.2143	94.5652	69.0476	50	100	95.6522
19	66.0714	45.1087	76.1905	56.5217	77.381	55.6159	98.2143	94.0217	72.0238	53.2609	98.8095	94.9275

Table 2: The percentage of correctly classified samples under the local roughness feature vector (F_1) using the Lab color model

b	L-Channel		a-Channel		b-Channel		Lab-Channels		gray-Channel		All-Channels	
	Training	Testing	Training	Testing	Training	Testing	Training	Testing	Training	Testing	Training	Testing
3	75	65.7609	77.381	63.0435	75	58.1522	97.619	87.6812	66.6667	57.4275	98.2143	90.5797
5	77.9762	60.8696	80.3571	66.3043	75.5952	59.7826	95.2381	88.7681	73.2143	54.529	95.8333	90.942
7	77.9762	63.0435	76.7857	63.2246	77.381	60.6884	95.8333	89.3116	73.8095	54.529	96.4286	89.4928
9	76.7857	62.3188	78.5714	64.4928	73.8095	63.2246	97.0238	89.6739	78.5714	55.9783	97.619	92.3913
11	73.8095	49.2754	82.7381	58.8768	69.4629	54.7101	97.619	88.2246	69.6429	48.7319	97.619	87.6812
13	72.0238	53.8043	77.381	55.2536	75	50.9058	98.2143	85.1449	67.2619	50	97.0238	87.1377
15	69.0476	53.8043	75.5952	54.1667	75	54.7101	98.8095	85.8696	64.2857	49.2754	98.2143	87.6812
17	35.119	27.3551	57.1429	45.1087	69.0476	52.5362	82.1429	72.2826	69.0476	50	97.619	86.413
19	36.9048	27.7174	57.1429	47.4638	69.6429	51.4493	80.9524	71.3768	72.0238	53.2609	99.4048	88.0435

Table 3: The percentage of correctly classified samples under the local roughness feature vector (F_1) using the HSV color model

b	H-Channel		S-Channel		V-Channel		HSV-Channels		gray-Channel		All-Channels	
	Training	Testing	Training	Testing	Training	Testing	Training	Testing	Training	Testing	Training	Testing
3	47.619	42.2101	61.9048	51.2681	71.4286	51.2681	85.119	72.4638	72.0238	61.9565	95.8333	87.3188
5	82.7381	61.5942	77.9762	56.8841	68.4524	48.3696	98.2143	91.1232	73.2143	54.529	97.619	85.3261
7	79.1667	64.4928	73.8095	55.7971	67.2619	52.5362	98.2143	91.4855	73.8095	54.529	96.4286	76.8116
9	83.3333	64.6739	75.5952	58.5145	69.0476	49.0942	97.619	91.2101	78.5714	55.9783	97.619	88.7681
11	75	61.2319	75	58.7868	73.2143	49.4565	97.619	89.1304	76.7857	51.6304	96.4286	86.5942
13	76.1905	63.0435	75	56.3406	72.4286	50.1812	98.2143	88.4058	73.8095	51.2681	97.0238	86.0507
15	76.1905	59.6014	75	51.6304	72.619	51.2681	95.8333	86.7754	71.4286	52.7174	97.619	85.3261
17	35.119	27.3551	57.1429	45.1087	69.0476	52.5362	82.1429	72.2826	69.0476	50	96.4286	76.8116
19	36.9048	27.7174	57.1429	47.4638	69.6429	51.4493	80.9523	71.3768	72.0238	53.2609	97.0238	78.442

Table 4: The percentage of correctly classified samples under the local contrast feature vector (F_2) using the RGB color model

d	R-Channel		G-Channel		B-Channel		RGB-Channels		gray-Channel		All-Channels	
	Training	Testing	Training	Testing	Training	Testing	Training	Testing	Training	Testing	Training	Testing
1	55.9524	40.3986	55.3571	48.3696	48.2143	32.4275	81.5476	64.1304	64.2857	40.942	85.119	65.5797
3	45.8333	41.8478	51.7857	43.2971	42.8571	29.1667	75	55.7971	50	36.7754	82.7381	57.0652
5	59.5238	40.0362	59.5238	40.0362	37.5	28.8043	67.2619	44.7464	47.619	36.9565	69.6429	47.8261
7	47.619	36.2319	50	37.6812	35.7143	27.3551	57.1429	46.9203	47.619	36.413	73.8095	46.1957
9	49.4048	39.1304	38.0952	32.971	37.5	26.6304	65.4762	40.5797	40.4762	36.7754	70.8333	43.6594

Table.5: The percentage of correctly classified samples under the local contrast feature vector (F_2) using the Lab color model

d	L-Channel		a-Channel		b-Channel		Lab-Channels		gray-Channel		All-Channels	
	Training	Testing	Training	Testing	Training	Testing	Training	Testing	Training	Testing	Training	Testing
1	51.1905	37.1377	56.5476	41.1232	57.1429	41.1232	99.4048	92.2101	64.2857	40.942	88.0952	62.8623
3	41.0714	37.5	33.1522	50	54.7619	38.587	73.2143	52.7174	50	36.7754	82.1429	59.9638
5	45.2381	36.413	40.4762	33.6957	53.5714	37.8623	67.8571	48.5507	47.619	36.9565	75.5952	51.6304
7	42.2619	28.6232	39.881	29.529	47.619	35.8696	64.2857	44.2029	47.619	36.413	71.4286	46.558
9	32.7381	26.6304	39.2858	25.3623	46.4286	38.4058	57.7381	40.2174	40.4762	36.7754	70.2381	47.4638

Table 6: The percentage of correctly classified samples under the local contrast feature vector (F_2) using the HSV color model

d	H-Channel		S-Channel		V-Channel		HSV-Channels		gray-Channel		All-Channels	
	Training	Testing	Training	Testing	Training	Testing	Training	Testing	Training	Testing	Training	Testing
1	56.5476	52.5725	39.881	34.4203	55.9524	40.5797	85.119	66.1232	64.2857	40.942	96.4286	85.6884
3	52.9762	36.5942	34.5238	29.1667	41.6667	41.3043	81.5476	61.413	50	36.7754	80.3571	65.5797
5	48.8095	34.7826	35.7143	26.6304	53.5714	38.9493	79.7619	58.3333	47.619	36.9565	84.5238	60.3261
7	48.8095	35.3261	34.5238	25.5435	48.8095	38.7681	71.4286	46.3768	47.619	36.413	75	52.1739
9	38.6905	30.4348	35.119	26.2681	47.0238	37.6812	63.6905	41.6667	40.4762	36.7754	75	43.6594

Table 7: The percentage of correctly classified samples under the local roughness and local contrast feature vectors {F_2, F_2} using the RGB color model (block size of the roughness are fixed on b=9)

d	R-Channel		G-Channel		B-Channel		RGB-Channels		gray-Channel		All-Channels	
	Training	Testing	Training	Testing	Training	Testing	Training	Testing	Training	Testing	Training	Testing
1	83.9286	66.1232	80.9524	61.5942	83.9286	65.0362	98.8095	83.6957	82.7381	61.413	98.8095	88.587
3	81.5476	64.4928	83.3333	63.7681	77.9762	59.058	99.4048	89.1304	79.7619	61.0507	98.8095	86.7754
5	77.381	59.9638	76.7857	60.8696	75	56.8841	98.8095	83.6957	78.5714	56.7029	98.2143	83.333
7	73.8095	57.4275	73.2143	56.7029	73.8095	51.087	95.2381	80.0725	74.1048	51.087	95.2381	80.6159
9	78.5714	53.6232	75.5952	52.1739	67.8571	47.2826	94.0476	74.2754	77.381	53.9855	96.4286	75.3623

Table 8: The percentage of correctly classified samples under the local roughness and local contrast feature vectors {F_2, F_2} using the Lab color model (block size of the roughness are fixed on b=9)

d	L-Channel		a-Channel		b-Channel		Lab-Channels		gray-Channel		All-Channels	
	Training	Testing	Training	Testing	Training	Testing	Training	Testing	Training	Testing	Training	Testing
1	84.5238	68.8406	84.5238	69.7464	88.0952	77.7174	100	92.2101	82.7381	61.413	97.619	88.5643
3	83.3333	65.0362	84.5238	69.7464	89.2857	78.9855	99.4048	90.0362	79.7619	61.0507	98.2143	90.942
5	74.4048	59.7826	79.1667	68.6594	84.5238	72.1014	97.619	88.4058	78.5714	56.7029	98.2143	89.6739
7	77.9762	58.6957	83.3333	61.5942	86.3095	74.6377	97.619	85.1449	74.1048	51.087	98.2143	89.3116
9	75.5952	55.7971	80.9524	63.587	83.9286	72.1014	95.8333	83.5145	77.381	53.9855	98.2143	83.5145

Table 9: The percentage of correctly classified samples under the local roughness and local contrast feature vectors {F_2, F_2} using the HSV color model (block size of the roughness are fixed on b=9)

d	H-Channel		S-Channel		V-Channel		HSV-Channels		gray-Channel		All-Channels	
	Training	Testing	Training	Testing	Training	Testing	Training	Testing	Training	Testing	Training	Testing
1	82.7381	58.8768	80.9524	63.0435	71.4286	54.8913	97.0238	82.2464	82.7381	61.413	96.4286	85.6884
3	76.1905	61.413	76.1905	58.8768	67.2619	55.0725	94.6429	77.3551	79.7619	61.0507	95.8333	86.0507
5	72.619	57.6087	72.619	54.1667	67.2619	52.3551	89.2857	69.7464	78.5714	56.7029	97.619	78.442
7	81.5476	48.0072	64.881	48.7319	62.5	47.4638	93.4524	61.2319	74.4048	51.087	94.0476	71.9203
9	75.5952	52.8986	70.2381	46.0145	65.4762	47.2826	82.1429	57.6087	77.381	53.9855	95.8333	64.8551

Table 10: The percentage of correctly classified samples under the local roughness and local contrast feature vectors {F_2, F_2} using the RGB and Lab color model (block size of the roughness are fixed on b=9)

RGB	Lab	Training	Testing
d	d		
1	1	100	94.7464
3	3	100	95.2899
5	5	100	92.2101
7	7	100	91.8478
9	9	100	8733188

Table 11: The percentage of correctly classified samples under the local roughness and local contrast feature vectors {F_2, F_2} using the RGB and HSV color model (block size of the roughness are fixed on b=9)

RGB	HSV	Training	Testing
1	1	0	92.9348
3	3	99.4048	91.4855
5	5	98.8095	90.2174
7	7	100	85.8696
9	9	98.8095	79.7101

Table 12: The percentage of correctly classified samples under the local roughness and local contrast feature vectors {F_2, F_2} using the Lab and HSV color model (block size of the roughness are fixed on b=9)

Lab	HSV	Training	Testing
d	d		
1	1	100	95.471
3	3	100	95.1087
5	5	99.4048	94.3841
7	7	99.4048	92.2101
9	9	98.8095	89.8551

Table 13: The percentage of correctly classified samples under the local roughness and local contrast feature vectors {F_2, F_2} using the RGB, Lab and HSV color model (block size of the roughness are fixed on b=9)

Lab	RGB	HSV	Training	Testing
d	d	d		
1	1	1	100	95.8333
3	3	3	99.4048	95.8333
5	5	5	100	95.1087
7	7	7	100	92.9348
9	9	9	100	90.7609